

HARPS Gets New Fibres After 12 Years of Operations

Gaspare Lo Curto¹
 Francesco Pepe²
 Gerardo Avila¹
 Henri Boffin¹
 Sebastian Bovay²
 Bruno Chazelas²
 Adrien Coffinet²
 Michel Fleury²
 Ian Hughes²
 Christophe Lovis²
 Charles Maire²
 Antonio Manescau¹
 Luca Pasquini¹
 Samuel Rihs²
 Peter Sinclair¹
 Stéphane Udry²

¹ ESO

² Université de Genève, Département d'Astronomie, Versoix, Switzerland

In June 2015, as part of the HARPS Upgrade 2 Agreement signed in 2013 between ESO and Geneva University, a new set of non-circular (octagonal) optical fibres, with improved mode-scrambling capabilities, has been installed. The motivation for the exchange of the fibre link and the results from the commissioning tests are presented. The throughput of the instrument (+40% at 550 nm), its illumination uniformity and stability, and thus its radial velocity (RV) stability, are significantly improved. An RV offset correlated with the width of the stellar lines is found with the new fibres from observations of RV standards. As a result of this major upgrade, and once the laser frequency comb that is already assembled in the HARPS room is fully functional, we expect to reach an RV precision better than 0.5 m s^{-1} on bright stars.

Rationale for a fibre upgrade

The High Accuracy Radial velocity Planet Searcher (HARPS) was developed between 2000 and 2003 to measure stellar radial velocities with a precision of 1 m s^{-1} or better (Mayor et al., 2003) and has proved to be a spectacularly successful workhorse spectrograph for the discovery and monitoring of extrasolar planets. The spectrograph is based on the simultaneous-reference technique

(Baranne et al., 1996), which has the great advantage with respect to the self-calibration technique (iodine absorption cell) of using the whole visible spectrum without any light loss and spectral contamination.

Since the simultaneous-reference technique relies on the stability of the instrumental profile (IP), at least on timescales of an observing night, the technique requires the use of optical fibres. They ensure that the stellar image injected into the fibre at the telescope focus is well scrambled, i.e., the light distribution at the fibre exit is homogeneous and does not change with time¹. However, an optical fibre only scrambles the near field (i.e., the light distribution on the fibre tip) in a satisfactory way, but not its far field (the angular distribution within the light cone leaving the fibre). It was therefore necessary to introduce the concept of a double scrambler — a set of two fibres connected by a simple optical system that exchanges the near field of the first fibre with the far field of the second fibre, and vice versa (Baranne et al., 1996). This fibre link ensures a good scrambling of both near and far field.

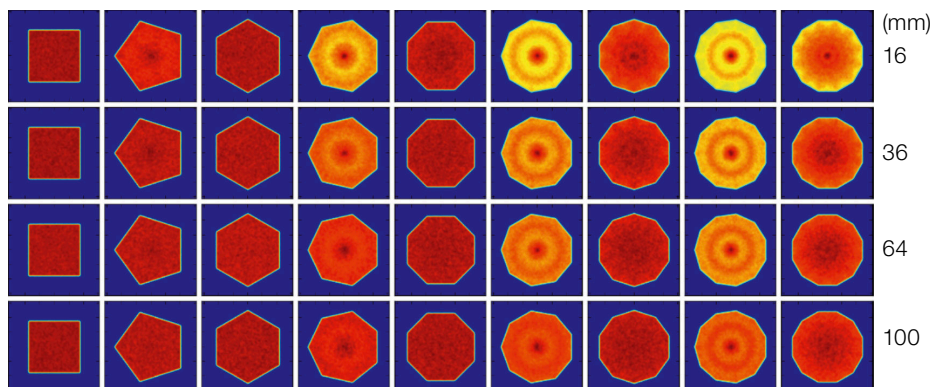
During the design phase of HARPS, and following tests on CORALIE, we could estimate the level of scrambling to be expected with HARPS (Pepe et al., 2002). It became clear that the scrambling alone would not be sufficient to achieve the 1 m s^{-1} requirement, and that a requirement on the centring precision of the star on the fibre during the scientific exposure had to be set. It was estimated, and confirmed, that a systematic de-centring of the stellar image to the fibre edge would induce an RV effect of the

order of 3 m s^{-1} (Mayor et al., 2003). While de-centring was addressed first by an improvement to the 3.6-metre guiding system, followed by the introduction of a tip-tilt system (Lo Curto et al., 2010), in the absence of other solutions this issue of imperfect scrambling has been accepted for many years.

It was already known that circular fibres carry some memory effect of the angular and spatial distribution of the injected light. However, only later it was understood that far-field changes dramatically impact the IP of the spectrograph in presence of optical aberrations (Perruchot et al., 2010). In the meantime, non-circular fibres had become available and it was demonstrated, by simulation and laboratory tests, that their scrambling efficiency is far superior to that of circular fibres (see Figure 1 and Chazelas et al. [2010], Figures 5 and 10).

On account of their advantages, octagonal fibres were quickly employed in SOPHIE (Bouchy et al., 2013) at the Observatoire de Haute-Provence and in the northern copy of HARPS at the Telescopio Nazionale Galileo (Cosentino et al., 2012) with excellent results. The improvement was so convincing that it was proposed that a copy of the HARPS-N fibre link on HARPS at the 3.6-metre telescope should be implemented within a new HARPS Upgrade 2

Figure 1. Near-field fibre scrambling (Zemax simulation) is shown as a function of fibre shape (horizontal axis) and fibre length (vertical axis). The output face of the fibre is shown in each case. The simulation assumes an input spot of $10 \mu\text{m}$ in diameter at the centre of the fibre with a core thickness of $100 \mu\text{m}$. Hexagonal, octagonal and square fibres show very good uniformity for lengths above 16 mm.



project (see Figure 2). The agreement between the Geneva Observatory and ESO also foresaw an upgrade of the HARPS data reduction pipeline, which was necessary to cope with the new laser frequency comb (LFC; Lo Curto et al., 2012) and the fibre upgrade, as well as an improvement of the thermal stability of the instrument and its maintenance for an additional three years.

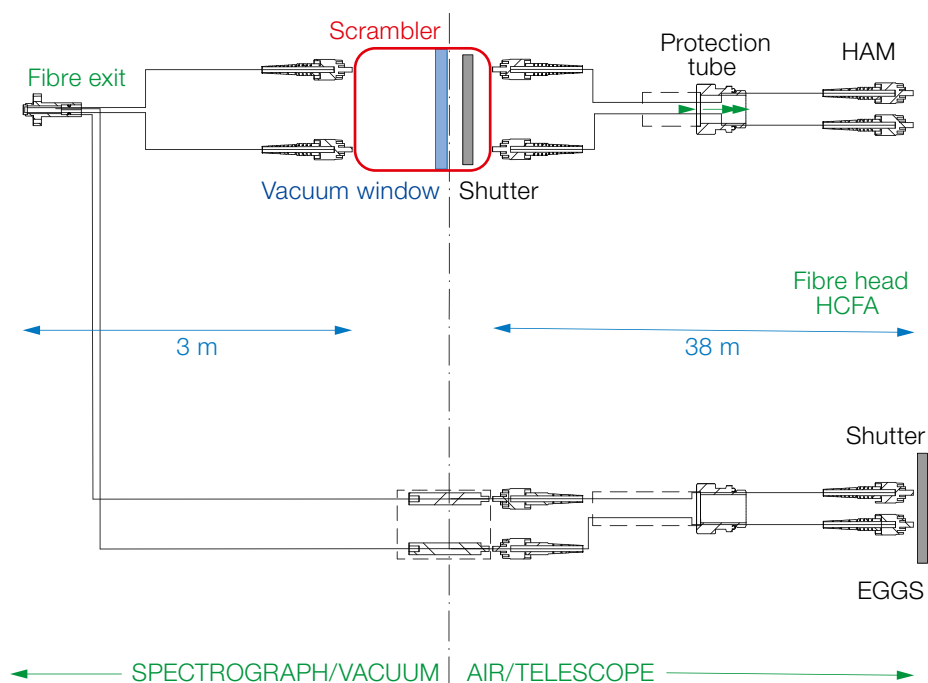
An optical fibre link is often considered as a necessary evil for the sake of precision. The original HARPS fibre link (40 metres of fibre and a double scrambler) achieves an efficiency of only about 55 % at peak, without taking into account additional slit losses occurring in poor seeing or with non-optimum telescope image quality. By harnessing the improved fibre technology, we had demonstrated on HARPS-N that the fibre-link efficiency could be improved to about 70 %, and that only about 10 % of the 30% loss was due to the double scrambler. For this reason, ESO and the Geneva Observatory agreed on a goal of 20 % relative efficiency improvement with respect to the old HAM (high accuracy mode) fibre link on HARPS at the 3.6-metre.

Together with the new fibre link (Figure 2), we also replaced the homemade HAM shutter with a commercial bi-stable Uniblitz shutter and developed a new miniaturised shutter for the high efficiency mode (EGGS) fibre head. Finally, to improve the functionality of the EGGS mode, the upgrade provided the opportunity to repair its broken sky (or simultaneous reference) fibre.

The HARPS Upgrade 2 Agreement also foresaw the update of the data-reduction pipeline, the installation of thermally controlled vacuum-vessel feet for better thermal stabilisation of the instrument, a new (spare) vacuum pump and other minor maintenance tasks on the instrument. All these aspects were successfully executed during the fibre upgrade mission.

A new fibre link

The new HAM fibre link is conceptually identical to the old fibre link (Mayor et al., 2003) with the only difference being the



use of octagonal fibres, instead of circular fibres (Figure 3), of the same effective diameter. The detailed mechanical and optical design of the fibre head, the scrambler and the fibre exit were copied from HARPS-N because of the slightly improved optical performance. On the fibre exit side, the EGGS fibres are integrated in the same ferrule and use the same relay optics as the HAM fibres. However, the EGGS fibres do not use a double scrambler. It would have been very difficult to safely handle a 40-metre long EGGS fibres and a vacuum feedthrough attached to the fibre exit and the HAM scrambler, while pulling the whole system through the telescope Coudé path and into the vacuum vessel. For this reason, we decided to split the EGGS fibres at the vacuum feedthrough and install fibre connectors on the external side of the vacuum flange. Furthermore, we changed the fibre head of EGGS in order to adopt the same solution and optics as for the HAM fibres. In addition to being easy to align, the new fibre-head optics of EGGS fibres now injects the stellar image instead of the telescope pupil into the fibre's near field. Since the pupil is stable by definition, and the near-field (stellar image) is perfectly scrambled by the octagonal fibre, we can also expect better radial velocity performance for the EGGS fibres.

Figure 2. Configuration of the fibre link for the HAM and EGGS fibre links from the telescope (fibre head) to the spectrograph (fibre exit).

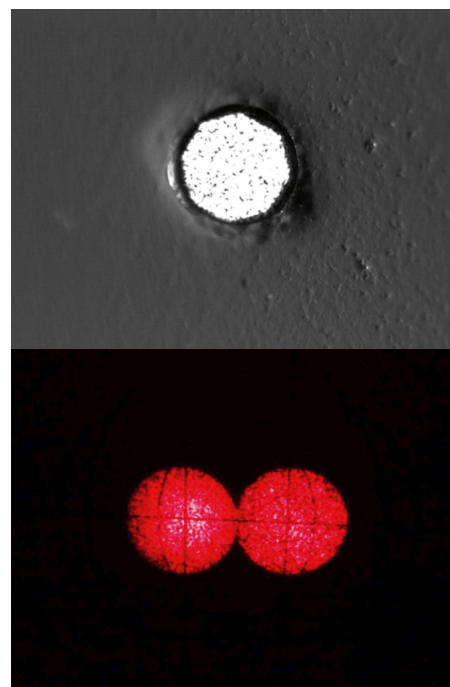


Figure 3. Top: Near-field image of the back-illuminated octagonal object fibre observed with a microscope through the 140 μm pinhole in the HARPS guiding mirror during alignment and focusing. Bottom: Far-field image of the back-illuminated fibres (object and sky fibre) during alignment of the optical axis.

A complete fibre link for HARPS, plus one set of spare fibres, was assembled, aligned and successfully tested in the laboratory with respect to total transmittance and focal ratio degradation (FRD). At La Silla, the optical alignment of the fibre-link optics was re-verified before installation (Figure 3). On 19 May 2015 HARPS stopped operations and the instrument was opened. Installation and alignment of the fibre link lasted roughly one week. On 29 May, the vacuum vessel was closed and evacuated for the last time. Finally, a formal commissioning of the new fibre took place, finishing on 3 June, when the instrument was handed back to Science Operations.

Table 1 shows laboratory measurements of the total efficiency and FRD of the two HAM fibres of the new fibre link, at three different wavelengths. The total throughput has been measured in nominal conditions, i.e., injecting a 3.6-metre telescope-like $F/8$ beam and measuring the total transmitted flux within the $F/7.5$ acceptance beam of the spectrograph. Values higher than 75 % were obtained in the green–red part of the spectrum, where the internal transmittance of the fibres is excellent. These values have to be compared to the 55 % total throughput measured for the original HARPS fibres in 2002.

The FRD indicates the fraction of the light falling within the $F/7.5$ cone compared to the total flux exiting the fibre. The values show that only about 6 % of the light falls outside the nominal acceptance cone. Such very low FRD losses are achieved when the fibres are prepared in a suitable way. Experience has shown that stress-free mounting is essential and can be obtained by using soft glue when connecting the fibres. Also, the thick cladding and buffer makes the fibre less sensitive to stress. Nevertheless, another aspect must be considered: the HARPS solution foresees gluing the relay lenses directly on to the fibre tip. By this means reflection losses are avoided and, even more important, the remaining surface defects on the fibre tip, which would produce stray light and FRD, are levelled out. Finally, after subtracting FRD losses and internal transmittance losses, less than 10 % loss can be assigned to the scrambler optics. In fact, most of the losses

Wavelength [nm]	Fibre A (object)		Fibre B (sky or simultaneous)	
	FRD	Throughput	FRD	Throughput
600	94.2%	79.8%	94.7%	79.3%
550	94.8%	77.3%	95.5%	76.8%
450	94.0%	68.4%	93.8%	66.2%

Table 1. Laboratory measurements of FRD and throughput of the new HAM fibres.

reported in the past occurred in the scrambler, and were due to the poor FRD of the first and long fibre section from a coupling-efficiency loss.

The scrambling power of the new fibres has been demonstrated to be a factor of at least ten times the value measured using circular fibres (Cosentino et al., 2012). Also, it has been shown that the far field was stabilised to much better than 10 % relative variation, even when moving the injected test light source from the centre to the edge of the fibre. Altogether, we expected (and demonstrated on HARPS-N) that any de-centring of the star on the fibre would result in an RV effect of less than 0.5 m s^{-1} .

Commissioning results

Spectral format, point spread function and resolution

The fibre upgrade project foresaw the opening of the vacuum vessel in order to access the vacuum side of the fibre link. The fibre link had been prepared to allow a plug-and-play installation, but nevertheless, the new fibre exit that defined the spectrograph slit had to be re-aligned and re-focused. The alignment was performed in such a way as to match the spectral format recorded by the science

detector (charge coupled device [CCD]) prior to the upgrade. This objective was indeed achieved within a couple of pixels in both spectral (dispersion) and spatial (cross-dispersion) directions. For the focus however, two iterations of evacuating and re-opening the vacuum vessel had to be performed in order to obtain a form of through-focus test and define the best focus position. The focus was physically adjusted by mechanically moving the fibre exit.

Figure 4 shows the result of the last through-focus procedure performed when the vacuum vessel had been evacuated for the last time before the restart of operations. The measurements show the full width at half maximum (FWHM) of the thorium–argon spectral lines recorded by the CCD at various locations both in Y (dispersion) and X (cross-dispersion). The values are minimum, and the curve becomes flat, towards 0 mbar, the pressure at which the spectrograph is operated, demonstrating that we had achieved optimum focus.

Another measure of the focus quality is shown in Figure 5, where the width of the spectral orders is plotted as a function of time. It can easily be seen that the orders became wider with time indicating a clear defocus of the instrument.

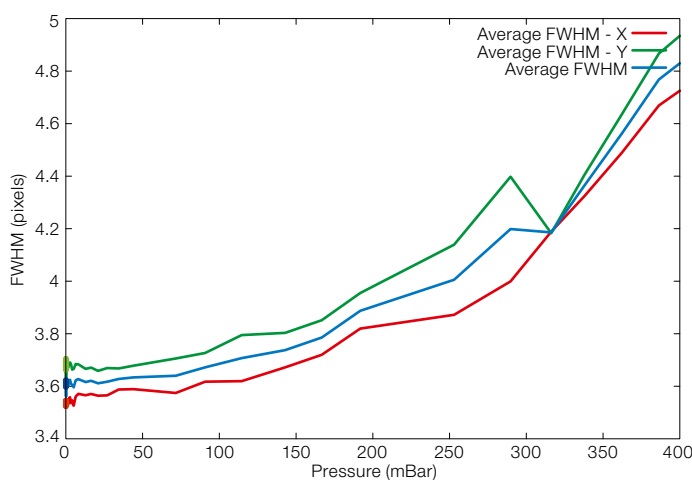


Figure 4. Through-focus of the new fibres as a function of vacuum pressure during the last evacuation of the vacuum vessel. At 0 mbar (operating condition), both the FWHM in dispersion and cross-dispersion direction are minimum and flat.

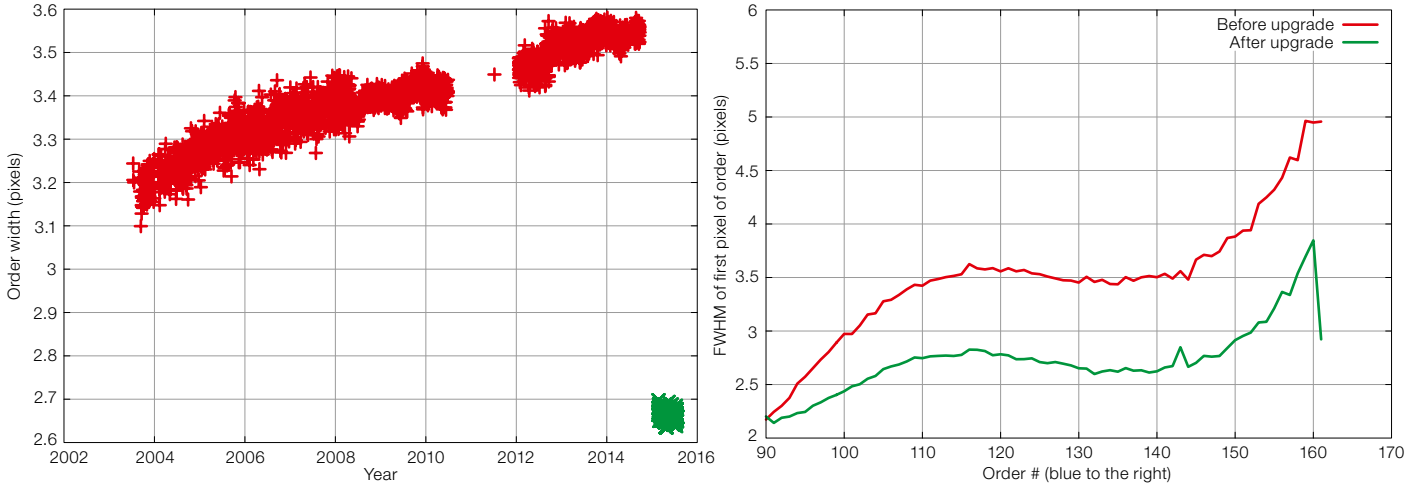


Figure 5. Width of the spectral orders measured at the CCD serial register are shown. Left panel: Time evolution for order #120. The width is measured by the online pipeline via a three Gaussian fit and recorded in the FITS header. Right panel: Order width as a function of order number before (19 May 2015) in red and after (29 May 2015) in green the intervention.

FWHM in dispersion direction showed that the focus was better on most locations across the CCD, but slightly worse on the centre-high part (red part) of the spectrum. The resulting (flux-averaged) resolving power remained almost unchanged (before: $R = 115\,000$; after: $R = 114\,000$). However, the homogeneity of the focus and the symmetry of the focus spots were greatly improved. This can be appreciated, for instance, by the right panel of Figure 5, which shows that the change of the spot size across the order is much smaller after the intervention and much closer to the expected anamorphic effect of the echelle spectrograph. Overall the focus and the homogeneity of the focal plane was improved by the intervention and the re-alignment. It is important to note that minor changes of the focal plane did not require develop-

ing a new version of the data-reduction pipeline. Nevertheless, significant work had to be invested to adapt the data-reduction system (DRS) to the slightly different spectral format and to cope with other changes, e.g., the altered flux calibration and the modified IP. An optimisation of the DRS to take best advantage of the new configuration is still in progress.

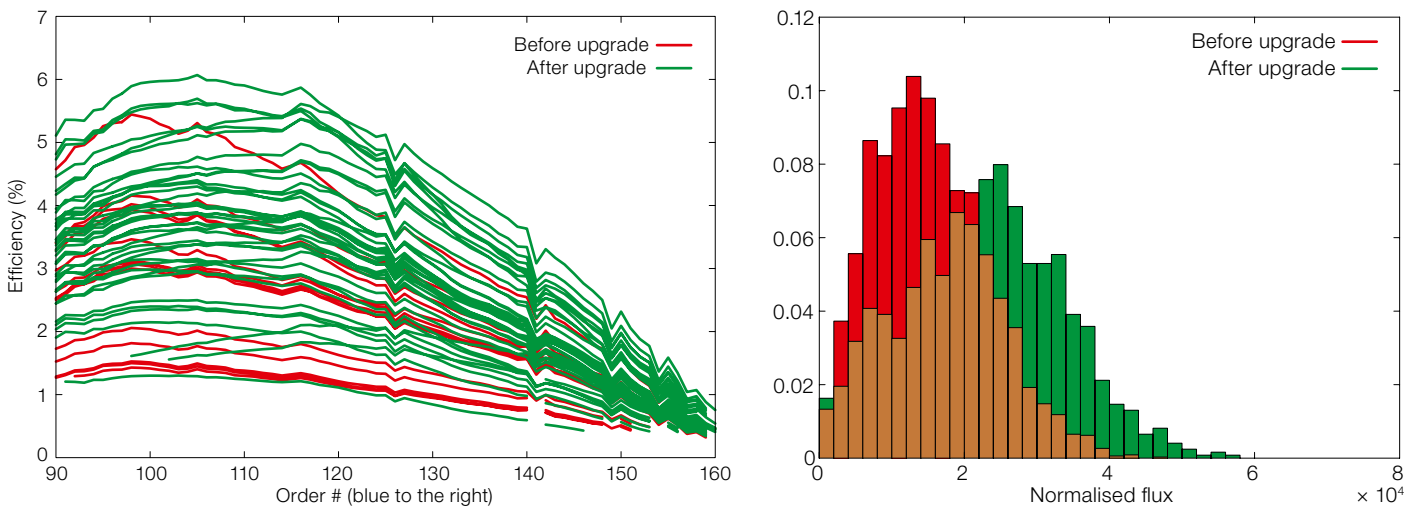
Throughput and efficiency

The increase in throughput was not one of the main motivations of this upgrade, however we expected a noticeable improvement given the experience gained with optical fibres, stress-free mounting

After the intervention (green points and line in Figure 5) the FWHM of the orders decreased considerably, demonstrating again the effectiveness of the focus procedure. The order width along a selected order is shown in the right panel of Figure 5, providing further evidence for the difference between pre- and post-intervention of the focus.

The improvement of the focus is not as dramatic in the dispersion direction as in the cross-dispersion direction. Nevertheless, a preliminary analysis of the

Figure 6. Left: Improvement of the overall instrumental throughput as measured from spectrophotometric standards. Right: Histogram of the direct comparison of the integrated flux (normalised by object magnitude and exposure time) of science targets.



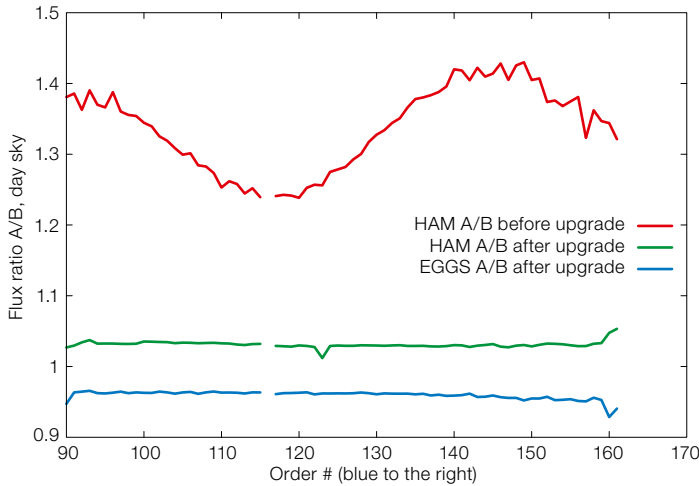


Figure 7. Fibre throughput ratio: science (A)/reference (B) integrated flux as measured from the diffuse light of the daytime sky. The curves obtained after the upgrade are very uniform and close to unity both for the HAM and the EGGS modes.

Before the upgrade, the throughput ratio between the two fibres of the HAM mode was about 1.35 and strongly colour dependent (Figure 7). After the upgrade, not only did the value get much closer to unity, but also the colour dependence had almost disappeared. In addition, by replacing the EGGS fibres, the broken fibre B of this mode was replaced. The flux ratio A/B for this mode was also measured and we obtained a value very close to unity and very uniform as a function of wavelength.

The same spectrophotometric standard stars as for the HAM efficiency measurement (Figure 6) were used to compare the efficiency of the HAM versus the EGGS mode. Figure 8 displays the efficiency of both modes at different air-masses. The seeing was about 1 arcsecond, and each EGGS spectrum was taken just after the HAM one, on the same target and without moving the telescope. The EGGS/HAM throughput ratio is shown in blue and is close to a factor of two. This is as expected given the larger fibre diameter (factor 1.4) and the absence of the image scrambler in the EGGS fibre link. It is interesting to note that the gain of EGGS versus HAM increases towards the blue, probably due to the fact that the effective seeing degrades towards the blue and the larger EGGS fibre is less affected than the smaller HAM fibre.

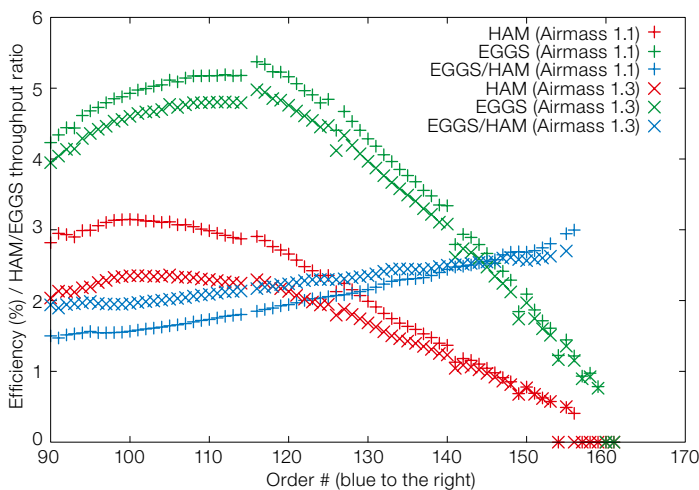


Figure 8. HAM & EGGS efficiency in % and relative EGGS/HAM throughput (on the same scale) are compared.

of fibre connectors, optical alignment and better injection optics. However, the gain had also to be demonstrated at the telescope. The efficiency was measured via observations of spectrophotometric standard stars. We collected about 20 spectra of standard stars within 2015 before, and 20 after, the intervention. The efficiency curves are shown in Figure 6 (left). The red curves are the efficiencies before the fibre link exchange, and the green curves after. The scatter is due to various atmospheric conditions, but the new curves are on average well above the old ones. From this dataset, we notice an approximately 40% average increase in efficiency at 550 nm for the new fibre link with respect to the old.

A more statistical way to demonstrate the efficiency gain, despite the short time basis, is to compare the flux of all

the stars of the HARPS Large Programme (PI: S. Udry) and the high-precision programme (PI: F. Pepe) observed before and after the upgrade. Figure 6, (right), shows the histogram of the integrated flux normalised by the stellar magnitude and the exposure time, before (red) and after (green) the upgrade. To avoid strong biases due to astroclimatic conditions, the period after the upgrade (1 June to 31 August 2015) was compared with the same period for the preceding year. The average efficiency appears to be as much as a factor of two higher. A more conservative estimate of the improvement is obtained by computing the ratio of the highest values, which should reflect the best-possible astroclimatic conditions in the two distributions. The resulting increase of 33% is consistent with that measured for the spectrophotometric standard stars, i.e., about 40%.

Effects of telescope decentring & defocus on the radial velocity

The main purpose of this upgrade was to install the new octagonal fibres to improve the scrambling of the spatial modes inside the fibres and in this way obtain a very uniform and stable light distribution at the exit of the fibre. The key performance indicator in this regard is the instrument sensitivity to de-centring. This indicator was evaluated before the upgrade by an RV drift of 3 m s^{-1} when de-centring the star by 0.5 arcseconds from the fibre centre. We repeated the same test after the upgrade and cannot detect any variation, down to the measurement uncertainty (Table 2). For each position of the star with respect to the fibre centre, we acquired three spectra and used the standard deviation (SD) of

Offset	ΔRV (m s ⁻¹)	SD(RV) (m s ⁻¹)	δRV (m s ⁻¹)
0.5" E	-0.22	1.19	0.52
0.5" W	0.05	0.90	0.42
0.5" N	0.13	1.54	0.87
0.5" S	-0.42	1.91	0.99

Table 2. Effect of de-centring on RV, measured on the star HD190248 with the HAM mode. The ΔRV s are measured with respect to the spectra acquired with the star centred on the fibre. The standard deviation (SD) over three acquired spectra is a better estimation of the RV uncertainty than the photon noise (δ), due to the intrinsic stellar RV jitter.

the measurements to express an uncertainty including the stellar jitter. The average RV offset is: $-12 \text{ cm s}^{-1} \pm 37 \text{ cm s}^{-1}$ (photon noise only, 12 data points); or $-12 \text{ cm s}^{-1} \pm 72 \text{ cm s}^{-1}$ (photon noise and stellar jitter included, 12 data points).

We have also measured RV variations with respect to changes of the telescope focus within a 0.6 mm range around its optimum position. In this case as well, RV variations are within the measurement uncertainty (the seeing was about 1 arc-second).

These are the main results achieved with this upgrade. Before, our RV precision was limited, by, among other factors, the centring of the star on the fibre. Even a small decentring of 0.05 arcseconds would give approximately a 30 cm s^{-1} effect on the RV measurement. This variation should be at least a factor ten lower, and small decentring or defocusing events, likely to happen during normal operations, will have now a negligible impact on the RV precision.

Radial velocity offset

By changing the fibres and re-adjusting the spectrograph focus, the IP of the spectrograph has changed significantly. Most of these changes are taken into account by the nightly wavelength calibration, which allows detection and correction of zero and first order effects on the radial velocity measurement introduced by a displacement or stretch of the focal plane. IP changes, however, especially if the IP is not perfectly symmetric, affect absorption and emission lines differently. An asymmetric IP may introduce a shift of the spectral line that depends on the

Star name	Spectral type	RV offset [m s ⁻¹]	Dispersion [m s ⁻¹]	CCF-FWHM [km s ⁻¹]	Mask used
HD109200	K1V	11.202	1.713	5.903	K5V
HD10700	G8.5V	15.935	1.509	6.287	G2V
HD1581	F9.5V	20.020	1.838	7.291	G2V
HD3823	G0V	17.488	2.449	7.252	G2V
HD20794	G8V	17.028	1.702	6.401	G2V
HD210918	G2V	16.145	1.622	6.858	G2V
HD26965A	K0.5V	16.732	2.017	5.927	K5V
HD177565	G6V	17.491	2.489	6.833	G2V
HD65907A	F9.5V	17.632	1.965	7.162	G2V
HD199288	G2V	14.124	1.739	6.509	G2V
HD207869	G6V	9.934	2.459	6.477	G2V
HD199604	G2V	15.916	1.946	6.643	G2V
HD210752	G0	14.371	1.745	6.665	G2V
HD55	K4.5V	15.297	2.178	6.049	K5V
GI87	M2.5V	0.736	2.043	3.687	M2V
HD154577	K2.5V	12.061	1.782	5.773	K5V
HD131653	G5	11.088	2.123	6.181	G2V
HD134088	G0V	11.637	1.802	6.388	G2V
HD147518	G4V	12.494	2.041	6.387	G2V
HD144628	K1V	11.599	1.768	5.873	K5V
GI588	M2.5V	-2.281	1.966	3.866	M2V

line width. For these reasons, we were expecting small RV offsets to be introduced by the new fibre link with respect to measurements prior to the upgrade.

We therefore observed a set of RV standard stars and compared their radial velocities before and after the upgrade. The results are summarised in Table 3 and show that such RV offsets indeed exist and are statistically significant. Furthermore, the offset is not a constant value for all stars. Indeed an effect due to IP changes and their interaction with the line width might be expected. This is confirmed by the data presented in Table 3, where the FWHM of the cross-correlation function (CCF) is shown together with the RV offset: the trend is for the RV offset to be smaller for narrower stellar lines. This trend implies that narrow stellar lines are affected by the IP change in a way similar to the (narrow) thorium–argon lines, such that the differential effect, and thus the RV offset, is small. For wider lines however, the differential effect is larger and thus the RV offset larger. Unfortunately the relation is not so well established, mainly because of stellar jitter and the fact that the CCF is a convolution of the stellar line width with the cross-correlation mask. The precise results depend also on the wavelength

Table 3. RV offsets measured for selected RV stable stars from various HARPS programmes. Column 4 lists the dispersion of the offset and column 5 the cross-correlation function FWHM for the particular mask used (column 6).

calibration algorithms and the data reduction in general. An in-depth study and optimisation of the wavelength calibration are underway. They are expected to lead to more quantitative results and a reduction of the observed offsets.

Prospects

A series of improvements to HARPS have been achieved with this latest upgrade: new fibre links, including new shutter systems; improved thermal stability; start of continuous operation of the vacuum pump; and vacuum-pump maintenance. The polarimetric optics have also been re-aligned to the new fibre link, and, consequent on the fibre change, we have improved the throughput and the RV precision of HARPS for both the HAM and the EGGs modes. On stellar targets a small RV offset is now observed after the change, and this offset is slightly different from star to star. We recommend users to consider the measurements before and after the upgrade as two dif-

ferent datasets, leaving an additional free parameter for the differential velocity of the two sets.

Once the laser frequency comb, which is already installed in the HARPS laboratory, becomes fully operational, we will be able to improve the wavelength calibration process significantly. As a result of these interventions, two of the most serious limitations, the illumination stability and the wavelength calibration, will have been solved. With HARPS we may then expect a long-term radial velocity precision of better than 50 cm s^{-1} and to achieve detection of a large number of super-earths in the habitable zone of Solar-type stars. Together with the upcoming Echelle SPectrograph for Rocky Exoplanet and Stable Spectroscopic Observations (ESPRESSO) instrument at the Very Large Telescope, HARPS promises to continue to be a pivotal player in

the exoplanet field, highly complementary to the upcoming space missions dedicated to extrasolar planets, such as the European Space Agency (ESA) CHaracterising ExOPlanet Satellite (CHEOPS), the US National Aeronautics and Space Administration (NASA) Transiting Exoplanet Survey Satellite (TESS) and the ESA PLANetary Transits and Oscillations of stars (PLATO).

Acknowledgements

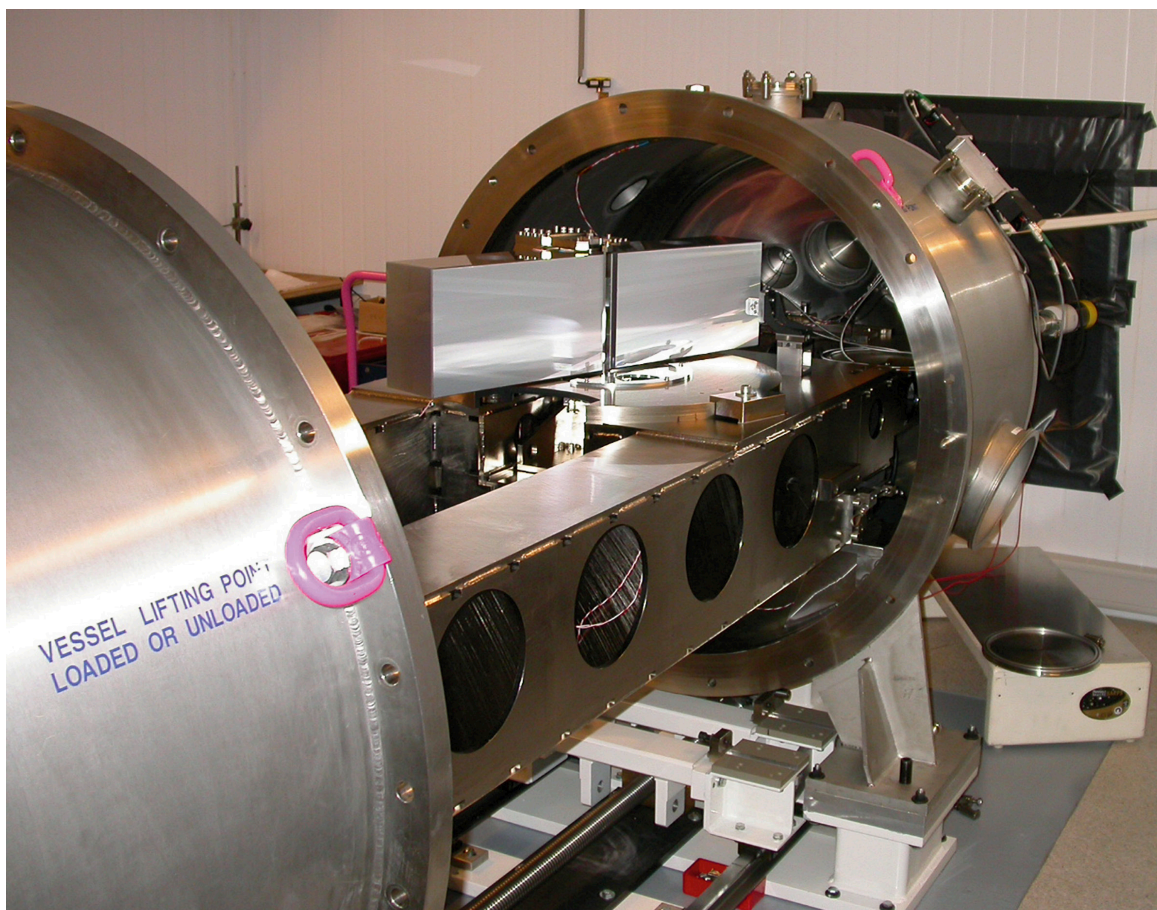
We acknowledge the enthusiastic support of the La Silla Observatory personnel and warmly thank the technical and the administrative personnel of the Geneva Observatory and everyone who contributed with enthusiasm and dedication to the success of the HARPS upgrade. Francesco Pepe acknowledges the Swiss National Science Foundation for the continuous support of this project through research grant Nr. 200020_152721. The presented work was executed under the HARPS Upgrade 2 Agreement between ESO and Geneva University.

References

- Baranne, A. et al. 1996, A&AS, 119, 373
- Bouchy, F. et al. 2013, A&A, 549, A49
- Chazelas, B. et al. 2010, Proc. SPIE, 7739E, 134
- Chazelas, B. et al. 2012, Proc. SPIE, 8450E, 13
- Cosentino, R. et al. 2012, Proc. SPIE, 8446E, 1V
- Lo Curto, G. et al. 2012, The Messenger, 149, 2
- Lo Curto, G. et al. 2010, Proc. SPIE, 7735E, 33
- Mayor, M. et al. 2003, The Messenger, 114, 20
- Pepe, F. et al. 2002, A&A, 388, 682
- Pepe, F. et al. 2002, The Messenger, 110, 9
- Perruchot, S. et al. 2011, Proc. SPIE, 8151E, 37

Notes

- ¹ A spectrograph forms a monochromatic image of the fibre tip on the detector. The fibre image defines the "slit" and thus the spectral resolution. A change of the fibre illumination would be seen as a change in the IP. If we consider that a spectral line has a width of 3 km s^{-1} at $R = 100\,000$, one understands that a small IP change can induce a line shift well above the 1 m s^{-1} precision goal.



The vacuum vessel of the High Accuracy Radial velocity Planet Searcher (HARPS) instrument open in the 3.6-metre telescope Coudé room, showing the optical bench and the diffraction grating.